Differences in the Stress Fibers between Fibroblasts and Epithelial Cells

JOSEPH W. SANGER, JEAN M. SANGER, and BRIGITTE M. JOCKUSCH
Department of Anatomy, School of Medicine, University of Pennsylvania, Philadelphia, Pennsylvania 19104; European Molecular Biology Laboratory, Heidelberg, Federal Republic of Germany. Dr. Jockusch's present address is Developmental Biology, University of Bielefeld, Federal Republic of Germany.

ABSTRACT In the stress fibers of two types of nonmuscle cells, epithelia (PtK_2, bovine lens) and fibroblasts (Gerbil fibroma, WI-38, primary human) the spacing between sites of α-actinin localization differs by a factor of about 1.6 as determined by indirect immunofluorescence and ultrastructural localization with peroxidase-labeled antibody. Both methods reveal striations along the stress fibers with a center-to-center spacing in the range of 0.9 μm in epithelial cells and 1.5 μm in fibroblasts. Periodic densities spaced at comparable distances are seen in PtK_2 and in gerbil fibroma cells when they are treated with tannic acid and examined in the electron microscope. In such cells, densities are found not only along stress fibers but also at cell-cell junctions, attachment plaques, and foci from which stress fibers radiate. These latter three sites all stain with α-actinin antibody on the light and electron microscope level. Stress fibers in the two cell types also vary in the periodicity produced by indirect immunofluorescence with tropomyosin antibodies. As is the case for α-actinin, the tropomyosin center-to-center banding is approximately 1.6 times as long in gerbil fibroma cells (1.7 μm) as it is in PtK_2 cells (1.0 μm). These results suggest that the densities seen in the electron microscope are sites of α-actinin localization and that the proteins in stress fibers have an arrangement similar to that in striated muscle. We propose a sarcomeric model of stress fiber structure based on light and electron microscopic findings.

Stress fibers, composed of bundles of aligned microfilaments, are a prominent feature of well-spread nonmuscle cells grown in culture (reviewed in reference 37), and are also present in at least some cells in situ (4, 43). Actin, myosin, tropomyosin, and α-actinin are each associated with stress fibers as determined by immunological labeling techniques (23, 25, 26, 41) and in the case of actin, by specific actin-binding agents as well (34, 44). The localization of myosin, tropomyosin, and α-actinin is in a banded pattern along the stress fiber analogous to patterns seen in the sarcomeres of striated muscle (7, 27, 28), whereas the pattern of actin distribution is usually (26) but not always (2, 13, 35) continuous along the fibers. Microinjection of fluorescently labeled proteins into living cells results in uniform distribution of fluorescence in the stress fibers when actin is injected (22, 38), but in banded distributions when either α-actinin (8, 21) or tropomyosin (42) is injected. Ultrastructural studies have shown that parallel arrays of actin filaments are aligned along the entire length of the stress fibers, with adjacent microfilaments often opposite in polarity to one another (2, 37). Myosin like filaments have also been detected (11, 29), as well as osmiophilic densities spaced along the fibers (10, 30, 32, 39). The ultrastructural densities are more prominent in cells treated with tannic acid and often appear to have a periodic distribution (12, 37). Spooner et al. (39) first noted the similarities between these densities in nonmuscle cells and the dense bodies of smooth muscle cells. Gordon (13) proposed that the densities were the sites of α-actinin localization, after comparing the immunofluorescence banding patterns due to myosin and α-actinin with the distribution of the densities. It has also been suggested that myosin is localized at the densities (12), and recently Herman and Pollard (15) have shown ferritin-labeled antimyosin localized on ultrastructural densities and, at lower concentration, between the densities, as well.

Here we demonstrate that the center-to-center spacings of α-actinin localization in stress fibers of fibroblasts differ by a factor of about 1.6 from those of epithelial cells. We exploited this new immunofluorescence information of cell type differences in α-actinin distribution to attempt to resolve the contro-

THE JOURNAL OF CELL BIOLOGY · VOLUME 96 APRIL 1983 961-969

versy over whether α-actinin or myosin is localized in the dense bodies in stress fibers. We compared the α-actinin immunofluorescence in different types of cells with the variation on an ultrastructural level in distribution of osmophilic densities and α-actinin antibody localization as determined with the peroxidase anti-peroxidase (PAP) method. These findings are discussed in terms of a sarcomeric model of stress fiber organization where α-actinin is localized in dense bodies.

MATERIALS AND METHODS

CELL CULTURES: PtK_2, WI-38, and gerbil fibroma cells were obtained from the American Tissue Type Collection (Rockville, MD). Bovine lens epithelial cells were obtained from Dr. Yves Courtois. The primary human fibroblasts were obtained from outgrowths of a human muscle biopsy. The cells were grown either on coverslips (to be used for subsequent immunofluorescence) or in 60-mm Falcon tissue culture dishes (Falcon Labware, Oxnard, CA to be used for electron microscopy). All the cells were grown in Eagle's medium supplemented with 1.5% glutamine, 10% fetal calf serum, and 1% antibiotic-antimycotic mixture (all

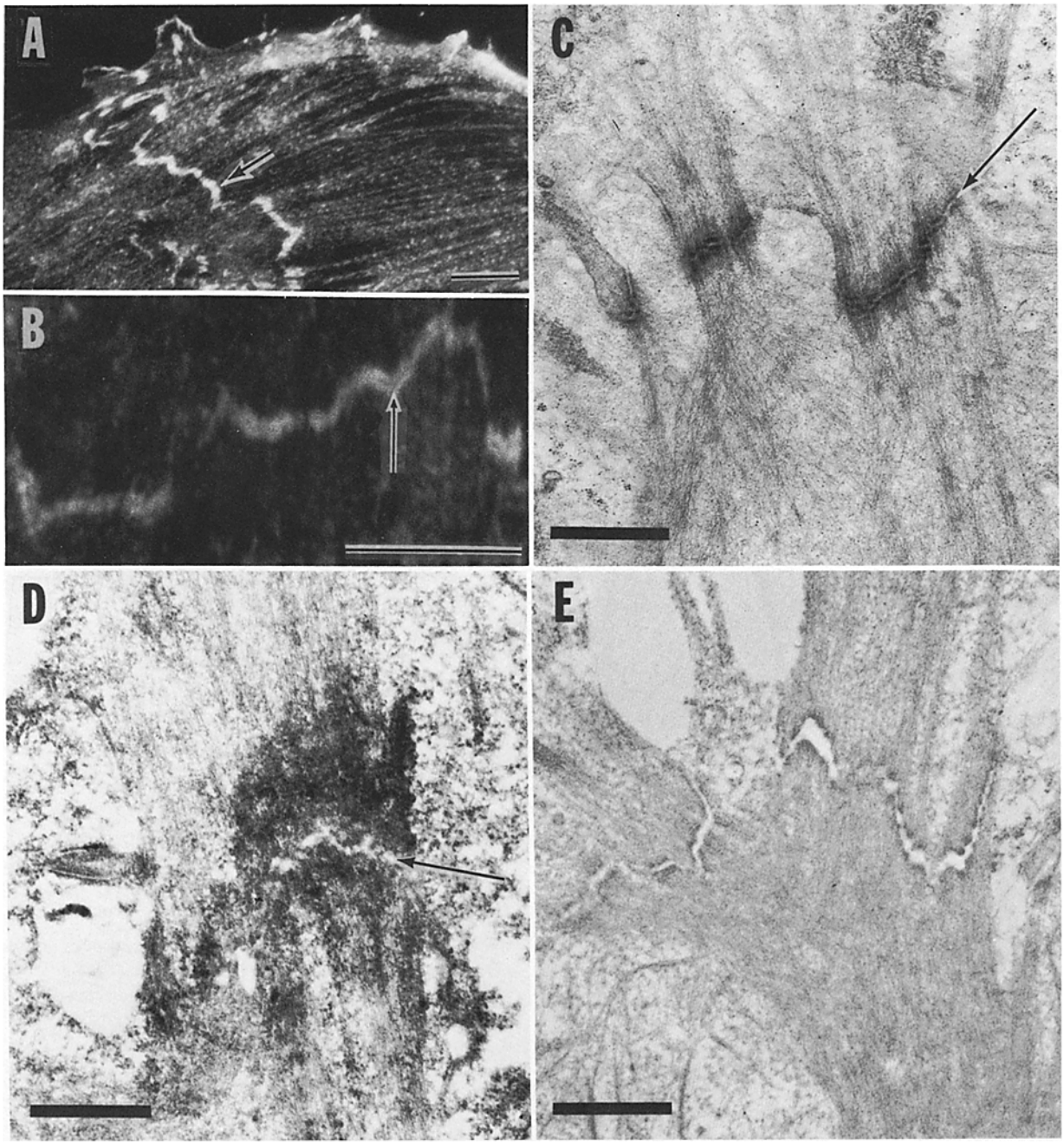

FIGURE 1 Different views of the intercellular junction between PtK_2 cells. (*A*) Two cells stained with α-actinin antibodies show a typical junction (arrow). Bar, 10 μm. × 1,000. (*B*) Higher magnification of the cellular junction in *A* to illustrate the gap in staining in the middle of the junction (arrow). Bar, 10 μm. × 2,600. (*C*) Electron micrograph of cellular junction in control cell. Note the extracellular gaps (arrow) and the density along the actin filaments near their attachment to the junctions. Bar, 1 μm. × 18,000. (*D*) Junction between cells that were treated with α-actinin antibodies and PAP antibodies. The extracellular gap (arrow) is visible as well as electron-dense deposits along the actin filaments attached to the junction. Bar, 1 μm. × 18,000. (*E*) Cells treated as in *D* but with α-actinin antibodies omitted from the process. No reaction product is found on the actin filaments. Osmiophilic staining is present along the junctional membranes. Bar, 1 μm. × 18,000.

obtained from Gibco Laboratories, Grand Island Biological Co., Grand Island, NY).

ANTIBODY AND FLUORESCENT HEAVY MEROMYOSIN PREPARATIONS: Affinity column purified antibodies against pig skeletal muscle α-actinin and chicken smooth muscle actin or tropomysoin were raised in rabbits or chickens and prepared as described previously (3, 16, 19, 20). Fluorescein-labeled heavy meromyosin was prepared as described previously (35).

FLUORESCENCE MICROSCOPY: Cells grown on coverslips were treated for immunofluorescence by fixation for 15–20 min at room temperature in 3% formaldehyde (prepared from paraformaldehyde) in standard salt (0.1 M KCl, 0.01 M KPO_4 buffer, 0.001 M $MgCl_2$, pH 7.0), rinses with standard salt, and permeabilization in 0.1% Nonidet P-40 (38). Reactions with antibody solution (against α-actinin, actin, or tropomyosin, 10–50 μg/ml) were carried out in moist chambers in a 37°C oven for 45 min, followed by rinsing and incubation with fluorescein- or rhodamine-labeled goat anti-rabbit or anti-chicken antibody for 45 min (38). For labeling actin with heavy meromyosin (HMM), 10–20 μl of fluorescein-labeled HMM (39) (0.5–1 mg/ml) was added to cells that had been permeabilized in cold acetone for 5 min and washed in standard salt. The cells were incubated in a moist chamber in the cold for ½ to 1 h, washed, then fixed in 3% formaldehyde in standard salt, washed again, and mounted either in Mowiol 4.88 (Farbwerke Hoechst, Frankfurt, Federal Republic of Germany) or glycerol.

Either a Zeiss Photomicroscope or an Olympus Vanox Microscope, both of which were set up for epifluorescence and equipped with a Zeiss 63X planapochromat lens, was used to observe cells. Micrographs were taken using Tri-X Pan film (Kodak) which was developed with Acufine or Diafine to obtain a 1000 to 1600 ASA rating.

Electron Microscopy

STANDARD PREPARATION: Cells grown on 60-mm Falcon tissue culture dishes were fixed for 30 min at room temperature with 2% glutaraldehyde in 0.1 M cacodylate buffer, pH 7.0, which contained 0.2% tannic acid. Cells were rinsed in the buffer and postfixed in 1% OsO_4 in 0.1 M cacodylate buffer, pH 6.0, for 20 min in the cold. After several rinses in buffer, the cells were exposed to 1% tannic acid in 0.1 M cacodylate buffer for 30 min at room temperature and then dehydrated in ethanol and embedded in Epon. Polymerized wafers of Epon were separated from the Falcon dishes, and selected areas of cells were cut from the wafer, glued onto blocks of Epon, and sectioned parallel to the substrate (42). Sections were stained in uranyl acetate and lead citrate.

PAP TECHNIQUE: Cells grown in 60-mm Falcon tissue culture dishes were fixed and treated under the same conditions as the cells on coverslips (see Fluorescence Microscopy), but with 20–40 μl of anti-α-actinin antibodies. After the incubation with the second antibody (goat anti-rabbit), the dishes were treated with peroxidase coupled to rabbit PAP (obtained from N. L. Cappel Laboratories, Cochranville, PA), fixed in glutaraldehyde, exposed to 0.03% H_2O_2 for 15 min, and then incubated in a fresh H_2O_2 solution containing a 0.33% solution of 3,3′diaminobenzoate-4HCl (DAB; obtained from Polysciences, Warrington, PA) (40). Within a few minutes, a dark reaction product began to appear in the cells. The reaction was allowed to proceed in the dark for 10 to 30 min and was then stopped by washing with 50 mM Tris solution in standard salt. Cells were further rinsed in 0.1 M sodium cacodylate, pH 6.8, before being exposed to 1% O_8O_4 in 0.1 M cacodylate buffer, pH 6.8, for 20 min in the cold (4°C), and processed as outlined above for standard electron microscopic preparation. Neither tannic acid, lead citrate, nor uranyl acetate was used on these PAP-treated cells. For controls, we used 40–60 μl of standard salt in substitution for the α-actinin antibodies. These controls were otherwise treated the same as the other PAP cells.

MEASUREMENT OF FLUORESCENT BAND PATTERNS: All cells prepared for immunofluorescence microscopy were photographed at the same magnification and the micrographs were printed to give a final enlargement of × 1,500. Using a scale subdivided into 0.1-mm spacings and a dissecting microscope set at × 7 magnification, we measured the distance between the center of one fluorescent band and the center of the adjacent fluorescent band. In contrast to center-to-center measurements which are independent of exposure time of negatives and prints, measurements of band lengths vary with exposure. To compare band lengths in different cell types, we used a fixed exposure time to ultraviolet illumination and printed the resultant negatives at identical exposure times.

RESULTS

Controls for Localization of α-actin with PAP Antibody

PtK_2 and bovine lens cells are epithelial cells that attach to one another to form interconnected sheets. Indirect immunofluorescence studies revealed a marked concentration of α-actinin antibody in the junctional areas (Fig. 1 *a*). High magnifications of junctions (Fig. 1 *b*) showed a broad trilaminar band consisting of two stained areas of equal width separated by a narrow dark band. This middle dark band presumably corresponds to the 200–400-Å gap observed in control PtK_2 cells fixed in a tannic acid–glutaraldehyde solution (Fig. 1 *c*). For 200–300 nm on either side of the junction there is densely staining material along the actin filaments (Fig. 1 *c*). The distribution of reaction product generated by using α-actinin antibody and the PAP method (Fig. 1 *d*) was often spread over an area wider than that occupied by the tannic acid-enhanced density of an untreated junctional area (Fig. 1 *c*), but the gap between adjacent cells in PAP-reacted cell cultures remained visible. If the primary antibody to α-actinin was omitted from the PAP procedure, only a slight osmiophilic density was visible along the membrane in the junctional area (Fig. 1 *e*).

Other areas of cells known from immunofluorescence studies (10) to contain α-actinin are ruffles and the focal contact at the ends of stress fibers on the ventral surface of the cell or at the edges of cells (Fig. 2 *a*). When the PAP procedure was used in conjunction with α-actinin antibody, dense deposits were found at focal contacts at cell edges (Fig. 2 *b*) and ventral surfaces as well as ruffles (not shown). These deposits were absent if α-actinin antibody was omitted from the procedure.

Stress Fibers

Five different cell types were processed for indirect immunofluorescence with α-actinin antibody: gerbil fibroma (Fig. 3 *a*), primary human fibroblasts (Fig. 3 *c*), WI-38 fibroblasts (not shown), bovine lens epithelial cells (Fig. 3 *b*), and PtK_2

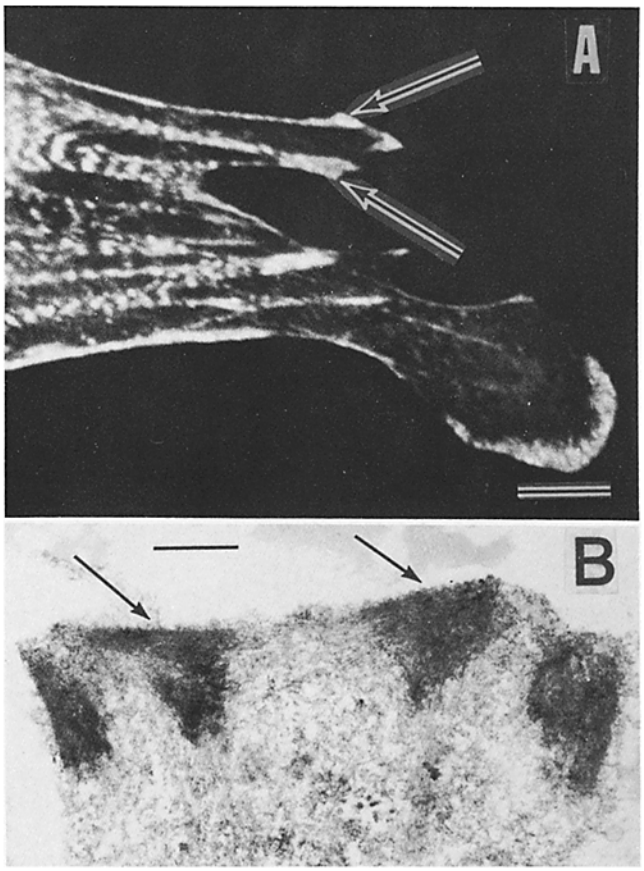

FIGURE 2 Focal contacts at edges of gerbil fibroma cells stained with α-actinin antibodies. (*A*) Fluorescent staining (arrows). Bar, 10 μm. × 1,100. (*B*) α-Actinin-PAP staining (arrows). Bar, 1 μm. × 11,400.

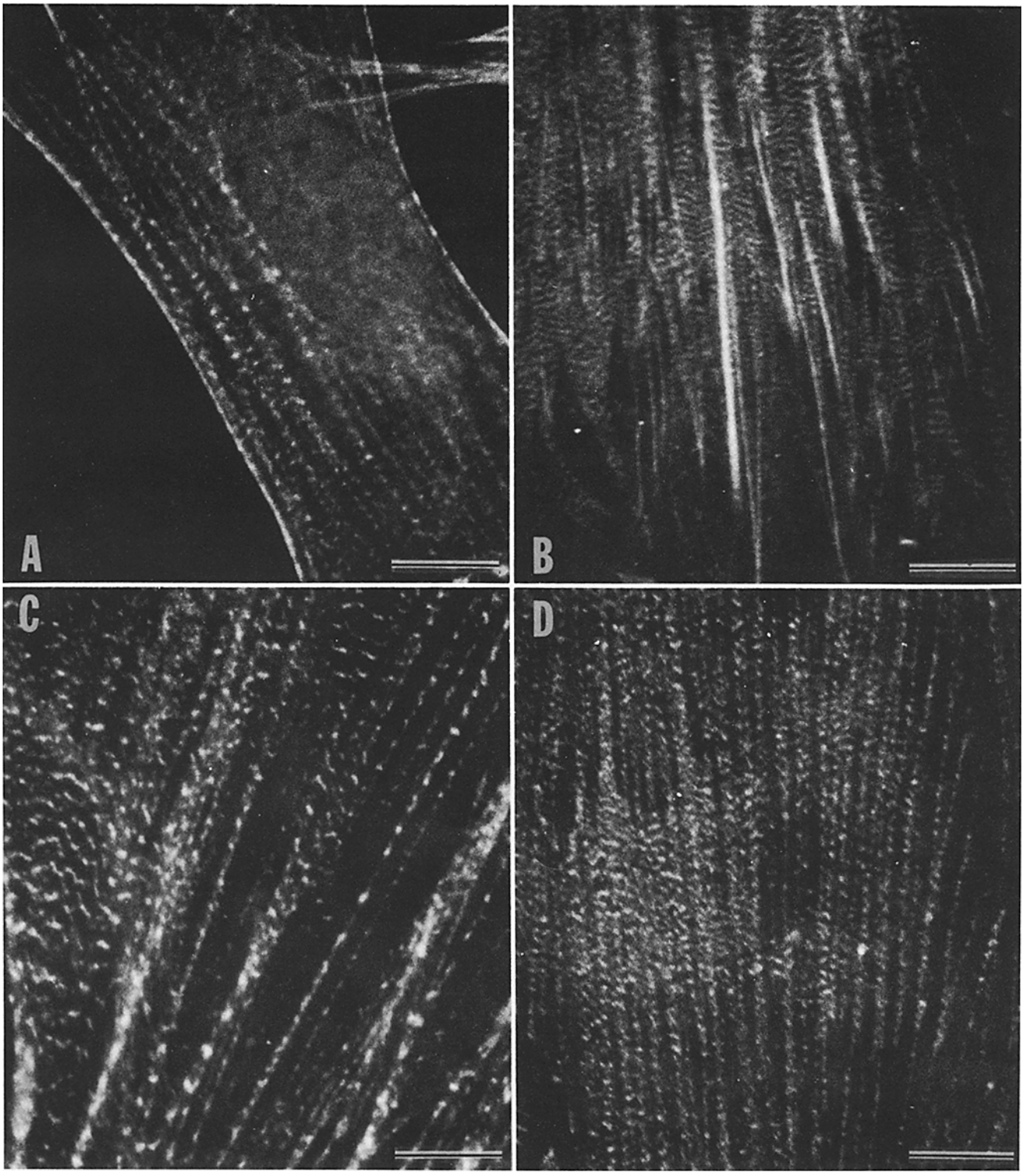

FIGURE 3 Four different cell types stained with alpha-actinin antibodies and photographed at the same magnification. Bar, 10 μm. × 1,850. (*A*) Gerbil fibroma cell. (*B*) Bovine lens epithelial cell. (*C*) Human fibroblast. (*D*) Rat kangaroo epithelial cell (PtK_2).

epithelial cells (Fig. 3*d*). Without measuring band patterns in the cells, it seemed apparent that the distance between fluorescent bands was appreciably shorter in the epithelial cells than in the fibroblastic cells, but that the length of the fluorescent bands was of the same magnitude in all the cells. Measurement of the center-to-center distance between fluorescent bands yielded the information in Fig. 4 and Table I. The average spacings in the fibroblastic cells (gerbil and human) were 1.5 and 1.7 μm, respectively, whereas the spacings in the two epithelial cell types (PtK_2 and bovine) averaged 0.9 and 0.8 μm, respectively. As indicated in Fig. 4 and Table I, there was a wide range in individual spacings within one cell line. This reflected differences between measurements on different stress fibers in the same and different cells as well as differences within the same stress fiber, although the latter was less common. The length of the fluorescent band itself averaged 0.4 μm

in all cells.

The stress fibers of cells treated with tannic acid during fixation for electron microscopy were characterized by osmophilic densities spaced along the fiber (Fig. 5). There was no morphological substructure of specialization within the stress fiber to account for the periodic densities and, in this respect, as well as in their association with actin filaments, the stress fiber densities resembled the densities seen at cell junctions (Fig. 1 *c*) and focal contacts (Fig. 2 *b*). Higher magnification electron microscopic images of dense bodies in both PtK_2 and gerbil (Fig. 6) cells revealed parallel dark filaments that were often continuous with thin filaments outside the dense bodies. The stress fiber densities were not spaced at precise intervals along the fibers (Fig. 5). To estimate an average distance between adjacent densities in a fiber, we counted the number of densities along segments of fibers 0.1 μm wide and 5–6 μm long. The average center-to-center spacing in PtK_2 was 0.6 μm and in gerbil 1.2 μm, values similar to the immunofluorescent banding described above (see Table I). The average length of individual densities was 0.2 μm for PtK_2 cells and 0.3 μm for gerbil fibroma cells.

PAP staining of cells incubated with anti-α-actinin produced periodic densities 0.3 to 0.5 μm in length, spaced 0.9–2.4 μm apart along stress of gerbil cells (Fig. 7 *a*). In PtK_2 cells (Fig. 7 *b*), similar-sized dense deposits were 0.5–1.1 μm apart. The average center-to-center spacings were 1.3 μm in gerbil cells and 0.8 μm in PtK_2 cells (Table I). No densities were visible when anti-α-actinin antibody was omitted from the procedure (Fig. 7 *c*).

Antitropomyosin Staining of Stress Fibers

It is known that tropomyosin is absent from areas of the cell containing α-actinin (13, 14, 24), but present between the bands of α-actinin in stress fibers (13). We predict, therefore, that fibroblasts that have longer center-to-center spacings of α-actinin than epithelial cells would also have longer center-to-

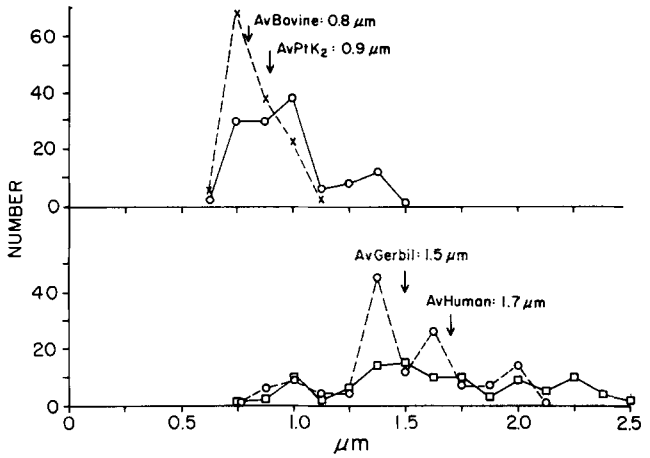

FIGURE 4 Distribution of center-center spacings of α-actinin staining patterns. The average values for each cell type are indicated. *Upper* panel, epithelial cells: (X) bovine; (○) PtK_2. *Lower* panel, fibroblasts: (○) gerbil; (□) human.

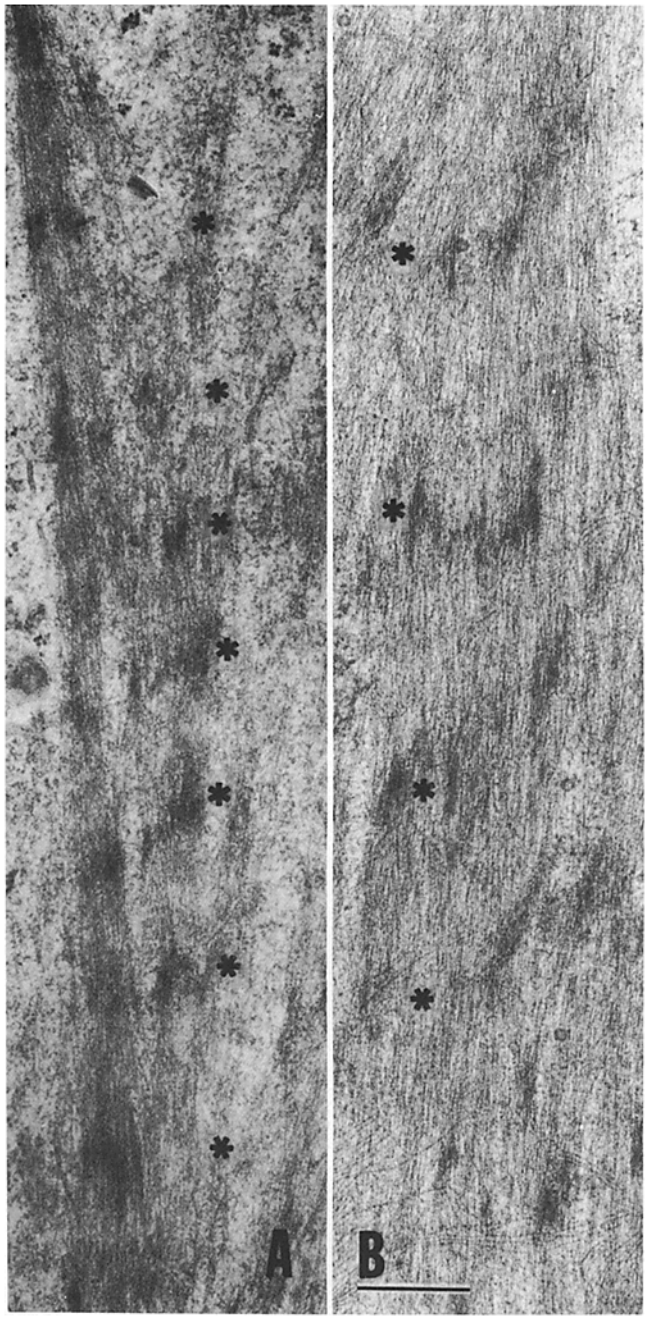

FIGURE 5 Normal electron micrographic appearance of dense bodies in (*A*) PtK_2 cells and (*B*) gerbil fibroma cells fixed with glutaraldehyde-tannic acid solutions. Asterisks have been placed at the level of the dense bodies. Bar, 0.5 μm. × 29,000.

TABLE I

Center-Center Spacings

	Fluorescent alpha-actinin antibody		Electron microscope densities		PAP α-actinin antibody	
	Average	Spread	Average	Spread	Average	Spread
	μm		μm		μm	
PtK_2	0.9	(0.6–1.5)	0.8	(0.5–1.1)	1.0	(0.7–1.4)
Gerbil	1.5	(0.75–2.1)	1.3	(1.0–2.4)	1.5	(0.9–2.5)

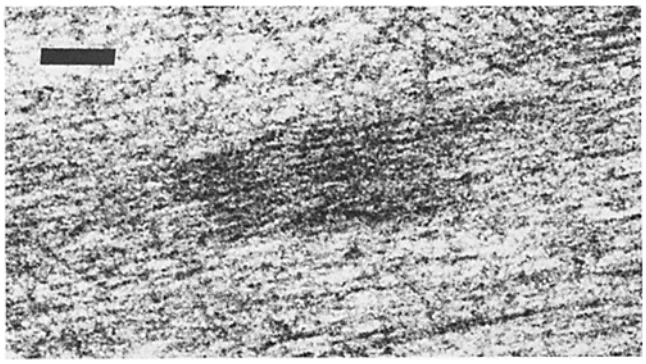

FIGURE 6 Higher magnification of a gerbil fibroma dense body shows the fibrous structure of the dense bodies. Bar, 0.1 μm. × 92,000.

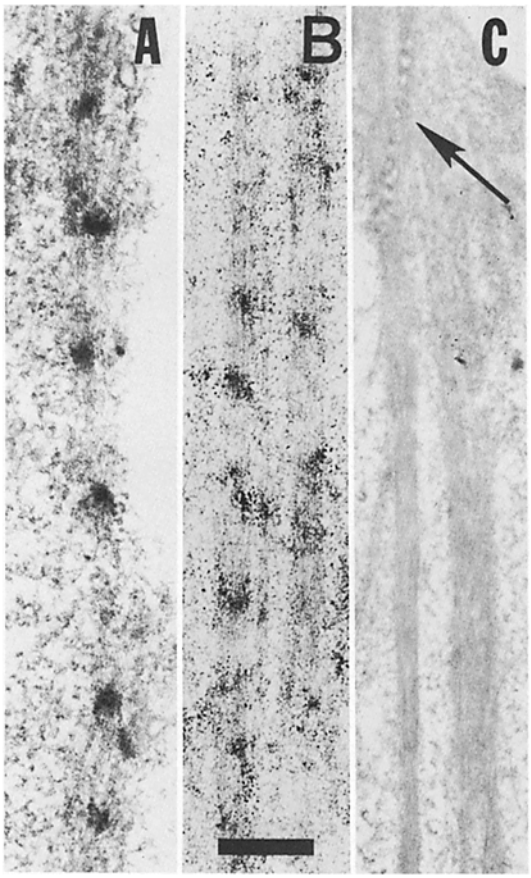

FIGURE 7 PAP-reacted stress fibers printed at the same magnification. Bar, 1 μm. × 11,000. (*A*) α-Actinin antibody-stained gerbil fibroma stress fiber. (*B*) PtK_2 stress fibers stained with α-actinin antibodies. (*C*) PtK_2 cells in which α-actinin antibodies were not used in the reaction. Note the lack of reaction product along the stress fibers and near the cellular junctions (arrow).

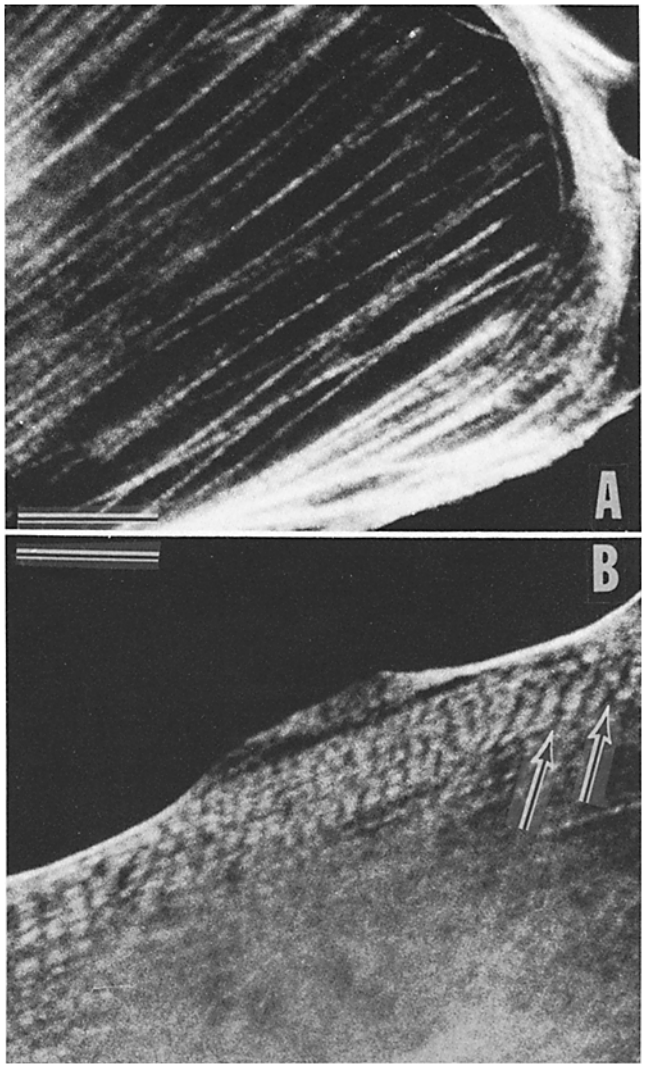

FIGURE 8 Fluorescent light micrographs of (*A*) PtK_2 cells and (*B*) gerbil fibroma cells stained with antibodies against tropomyosin. Bar, 10 μm. × 1,850. Note the closely spaced fluorescent bands in (*A*) PtK_2 cells versus the more widely spaced bands in (*B*) gerbil fibroma. The irregular shape of unstained areas (arrows) in the gerbil cells is similar to the irregular shape of the dense bodies in Fig. 5 *b*.

TABLE II

Tropomyosin Measurements

	Center-center distance		Length of stained band	
	Average	Spread	Average	Spread
	μm		μm	
PtK_2	1.0	(0.5–1.6)	0.6	(0.3–0.9)
Gerbil	1.7	(1.1–2.2)	1.2	(0.6–1.7)

center spacings of tropomyosin. This was true for gerbil fibroma (Fig. 8 *a*), primary human fibroblasts and WI-38 fibroblasts, all of which had longer center-to-center spacings of antitropomyosin staining than PtK_2 cells (Fig. 8 *b*) (Table II). Although the actual widths of the fluorescent bands are in part a function of the length of exposure of negative and prints, when these times are held constant for micrographs of the two types of cells a comparison of average widths can also be made. Under such conditions, antitropomyosin-stained bands were wider in gerbil fibroma cells than in epithelial cells (Table II). This is expected in view of earlier studies showing that double labeling with anti-α-actinin and antitropomyosin results in solid staining along stress fibers (13).

DISCUSSION

The results presented in this paper show that the average center-to-center distances along stress fibers between bands of

α-actinin, localized by indirect immunofluorescence, are greater in fibroblastic cells than in epithelial cells. On the electron microscopic level, the distance between bands of α-actinin, localized by α-actinin antibody and PAP, are comparable to the immunofluorescence measurements. The sizes of individual bands of PAP staining, however, are approximately the same in the two cell types. When used in conjunction with α-actinin antibody, PAP staining is also localized in focal adhesions and junctions, sites where immunofluorescence studies have shown that α-actinin is localized (24, 25). In electron micrographs of normally fixed cells, osmiophilic densities ~0.2 μm wide are found along the stress fibers separated by center-to-center distances similar to those found with α-actinin antibodies. Osmiophilic densities are also found in these cells at focal adhesions and junctions between cells.

Published immunofluorescence data indicate that myosin and tropomyosin are co-localized and are adjacent to sites of α-actinin localization along the stress fiber (13, 45). The osmiophilic densities in electron micrographs, then, could be sites either of myosin and tropomyosin or of α-actinin. The close correspondence, in two different cell types, between α-actinin banding and osmiophilic density banding leads us to suggest that α-actinin is localized in the densities. Herman and Pollard (15) using ferritin-coupled myosin antibodies found a higher concentration of ferritin grains associated with dense areas of HeLa stress fibers but also significant numbers of grains between the densities. Our model (Fig. 9) predicts that the grains should have been found only between the densities. To explain this discrepancy, we would like to make the following suggestions: It may be that the densities seen associated with ferritin by Herman and Pollard (15) were an artifact created by the addition of antimyosin at fairly high concentrations. In this case, according to our model, they would be located between the osmiophilic densities seen in normally fixed cells. We (J. W. Sanger and J. M. Sanger, unpublished observations) found that the latter are very sensitive to the condition of fixation and thus may not have been conserved well enough to stand out as distinct structures between the antimyosin created densities.

In sarcomeres of fast striated muscle, actin filaments are attached at one end to the Z-bands and tropomyosin binds along the actin filament except at the ends where actin is attached in the Z-bands. The distance between Z-bands, where α-actinin is localized, represents sarcomere length and is a function of the degree of contraction or stretch of the muscle. Bands of α-actinin are spaced closer together in contracted muscle than they are when the same muscle is stretched. At rest length, almost all vertebrate striated muscles have a sarcomere length of ~2.3 μm. The myosin and actin filaments are each also of uniform length in vertebrate striated muscle, 1.5 and 1.0 μm, respectively. In invertebrate striated muscle, there is much more variability. Sarcomere rest length can range from 0.9 μm in the subumbrellar muscle of jellyfish (5) to ~30 μm in the proventricular muscle of syllid worms (6). Myosin and actin filament lengths vary accordingly with lengths of 0.6 and 0.4 μm in the jellyfish muscle (5) and ~25 and 14 μm in the syllid worm muscle (6). Within one invertebrate animal, different muscles often differ in sarcomere rest length and myosin filament length as seen in the moth (33, 36) (Table III). Even within one muscle fiber, sarcomere rest length can vary (9, 31).

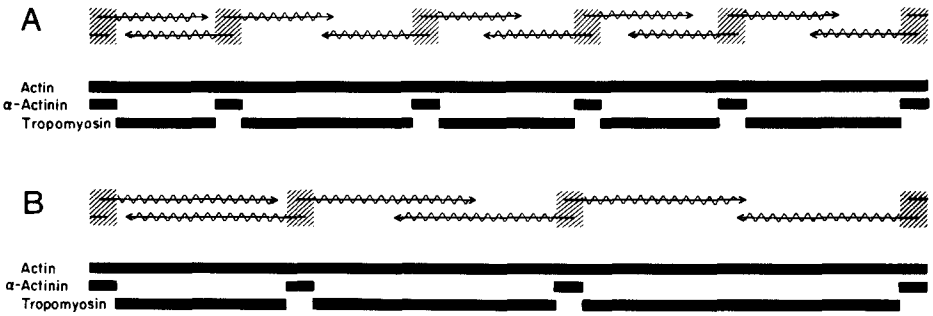

FIGURE 9 Comparison of the staining patterns (solid bars) produced by actin, α-actinin, and tropomyosin antibodies in two different cell types, (*A*) PtK_2 and (*B*) gerbil fibroma. Above the bars is a schematic model of a stress fiber that attempts to correlate the protein localization patterns with stress fiber ultrastructure. Actin filaments (→) are shown embedded in (and probably cross-linked by) α-actinin-containing dense bodies (cross-hatched rectangles). Regions of actin filaments projecting out of the dense bodies lack α-actinin but bind tropomyosin (wavy line) instead. Actin filament polarity is assumed to be in the direction indicated by the arrows.

TABLE III

Variations in Sarcomere, Thick Filaments, and Thin Filaments

Animal	Muscle	Rest length sarcomere	Thick filaments	Thin filaments	References
		μm	μm	μm	
Rabbit	Psoas	2.3	1.5	1.0	19
Frog	Sartorius	2.3	1.5	1.0	19
Jellyfish	Subumbrellar	0.9	0.6	0.4*	5
Syllid worm	Proventricular	30.0	25	14*	6
Moth	Cardiac	2.2	1.8	1.0*	36
	Flight	3.6	3.3	1.5*	33
	Alary	6.4	5.5	3.0*	36

* Actin lengths obtained by measuring filaments in sectioned material from published micrographs.

The model in Fig. 9 illustrates how a stress fiber in PtK_2 or gerbil fibroma cells may be constructed based on our light and electron microscopic findings. We used center-to-center spacings of α-actinin of 0.7–1.1 μm for PtK_2 and 1.1–1.9 μm for gerbil fibroma cells (Table I). In both cells, the actin filaments are shown inserted into the dense bodies which would be the sites of α-actinin localization. That region of the actin filament which is embedded in (or cross-linked by) α-actinin would be devoid of tropomyosin. We have used a uniform length of 0.6 μm for actin filaments of PtK_2 cells based on average measurements reported by Sanger and Sanger (37), and a uniform length of actin filaments, 1.0 μm for gerbil cells. This value yields the best fit of the center-to-center distance of α-actinin and is consistent with the continuous staining for actin which we observed. In addition, the observation of adjacent oppositely polarized actin filaments in stress fibers (2, 37) is consistent with the overlap proposed in the model. When comparing PtK_2 with gerbil fibroma cells, the length of the tropomyosin containing bands is a function of the extent of overlap as well as of length of the individual actin filaments. Shortening or lengthening of the stress fiber model would result in shorter or longer center-to-center spacing of α-actinin and tropomyosin staining. Since several other workers have demonstrated that myosin and tropomyosin are co-localized (13, 45), we assume that myosin will be in the area between the sites of α-actinin. If this were so, then the center-to-center spacings of myosin-positive bands should be larger in gerbil than in PtK_2 cells. Preliminary work with antimyosin staining is consistent with this prediction (J. W. Sanger, J. M. Sanger, and V. Nachmias, unpublished observations).

The only major differences between this sarcomeric model of the stress fiber and a classical vertebrate fast muscle sarcomere (18) are the interpositional stacking (1) of actin in the dense bodies and the overlap region of actin filaments between the dense bodies in the stress fibers. Although actin filaments of vertebrate fast muscle do not penetrate the Z-band, there is an interposition of actin filaments from neighboring sarcomeres in the Z-bands of insect muscles (1). While overlap regions of actin certainly occur in muscles (17), most muscles are stretched and held under tension during fixation to ensure a better alignment of the filaments and to reveal the H-zone. Perhaps if one could develop methods of stretching stress fibers before fixation, gaps between oppositely polarized actin filaments would be detected as well in stress fibers.

The different α-actinin periodicities reported for the stress fibers of the nonmuscle cells in this paper may represent different degrees of contraction and/or stretch of the fibers or may reflect the sort of sarcomeric variability seen in invertebrate striated muscles (Table III). Since the majority of the epithelial stress fiber periodicities due to α-actinin are spaced 0.8–0.9 μm apart, whereas the majority of α-actinin bands in the fibroblastic cells are 1.4–1.7 μm apart, we propose that there is a difference in the two cell types equivalent to the variability found in sarcomere rest length in different invertebrate muscles (Tables III). We predict that actin filaments, and perhaps myosin filaments as well, will be longer in the fibroblastic cells than in the epithelial cells. The variation in α-actinin banding that occurs within one cell and sometimes within one fiber would be more likely to be due to different degrees of contraction or stretch but could also be due to inhomogeneity in lengths of component filaments in the fibers as is observed in some individual vertebrate (31) and invertebrate (9) striated muscles.

We thank Drs. Yves Coutois and F. G. I. Jennekens for the generous gifts of bovine lens epithelium and the human biopsy sample.

One of the authors (Dr. Joseph W. Sanger) is expecially indebted to the generous and understanding support of the Alexander von Humboldt Stiftung. This research was also supported by grants from the National Institutes of Health (HL-15835 to the Pennsylvania Muscle Institute and GM 25653 to Joseph W. Sanger) and the Deutsche Forschungsgemeinschaft (Jo 55/.9 to B. M. Jockusch).

Received for publication 28 May 1982, and in revised form 2 December 1982.

REFERENCES

1. Ashhurst, D. E. 1967. Z-line of the flight muscle of belostomatid water bugs. *J. Mol. Biol.* 27:385–389.
2. Begg, D. A., R. Rodewald, and L. I. Rebhun. 1978. The visualization of actin filament polarity in thin sections. *J. Cell Biol.* 79:846–852.
3. Boschek, C. B., B. M. Jockusch, R. R. Friis, R. Back, E. Grundmann, and H. Bauer. 1981. Early changes in the distribution and organization of microfilament proteins during cell transformation. *Cell.* 24:175–184.
4. Byers, H. R., and K. Fujiwara. 1982. Stress fibers in cells *in situ*: immunofluorescence visualization with antiactin, antimyosin, and anti-alpha-actinin. *J. Cell Biol.* 93:804–811.
5. Chapman, D. M., C. F. A. Pantin, and E. A. Robson. 1962. Muscle in coelenterates. *Rev. Can. Biol.* 21:267–278.
6. del Castillo, J., M. Anderson, and D. S. Smith. 1972. Proventriculus of a marine annelid: muscle preparation with the longest recorded sarcomere. *Proc. Natl. Acad. Sci. USA.* 69:1669–1672.
7. Endo, M., Y. Nononaura, T. Masaki, I. Ohtsuki, and S. Ebashi. 1966. Localization of native tropomyosin in relation to striation patterns. *J. Biochem.* 60:605–608.
8. Feramisco, J. R. 1979. Microinjection of fluorescently labeled alpha-actinin into living fibroblasts. *Proc. Natl. Acad. Sci. USA.* 76:3967–3971.
9. Franzini-Armstrong, C. 1970. Natural variability in the length of thin and thick filaments in single fibres from a crab, *Portunus depurator*. *J. Cell Sci.* 6:559–592.
10. Giacomelli, F., J. Wiener, and D. Sprio. 1970. Cross-striated arrays of filaments in endothelium. *J. Cell Biol.* 45:188–192.
11. Goldman, R. D. 1972. The effect of cytochalasin B on the microfilaments of baby hamster kidney (BHK-21) cells. *J. Cell Biol.* 52:246–254.
12. Goldman, R. D., B. Chojnacki, and M.-J. Yerna. 1979. Ultrastructure of microfilament bundles in baby hamster kidney (BHK-21) cells: the use of tannic acid. *J. Cell Biol.* 80:759–766.
13. Gordon, W. E. 1978. Immunofluorescent and ultrastructural studies of "sarcomeric" units in stress fibers of cultured non-muscle cells. *Exp. Cell Res.* 117:253–260.
14. Gordon, W. E., and A. Bushnell. 1979. Immunofluorescent and ultrastructural studies of polygonal microfilament networks in respreading non-muscle cells. *Exp. Cell Res.* 120:335–348.
15. Herman, I. M., and T. D. Pollard. 1981. Electron microscopic localization of cytoplasmic myosin with ferritin-labeled antibodies. *J. Cell Biol.* 88:346–351.
16. Hoessli, D., E. Rungger-Brändle, B. M. Jockusch, and G. Gabbiani. 1980. Lymphocyte α-actinin. *J. Cell Biol.* 84:305–314.
17. Huxley, H. E. 1961. The contractile structure of cardiac and skeletal muscle. *Circulation.* 24:328–335.
18. Huxley, H. E. 1972. Molecular basis of contraction in cross-striated muscle. *In* The Structure and Function of Muscle. 2nd Edition. G. H. Bourne, editor. Academic Press, New York. II (Pt. 2):302–387.
19. Jockusch, H., B. M. Jockusch, and M. M. Burger. 1979. Nerve fibers in culture and their interactions with non-neural cells visualized by immunofluorescence. *J. Cell Biol.* 80:629–641.
20. Jockusch, B. M., K. H. Kelley, R. K. Meyer, and M. M. Burger. 1978. An efficient method to produce specific anti-actin. *Histochemistry.* 55:177–184.
21. Kreis, T. E., and W. Birchmeier. 1980. Stress fiber sarcomeres of fibroblasts are contractile. *Cell.* 22:555–561.
22. Kreis, T., K. H. Winterhalter, and W. Birchmeier. 1979. *In vivo* distribution and turnover of fluorescently labeled actin microinjected into human fibroblasts. *Proc. Natl. Acad. Sci. USA.* 76:3814–3818.
23. Lazarides, E. 1975. Tropomyosin antibody: the specific localization of tropomyosin in nonmuscle cells. *J. Cell Biol.* 65:549–561.
24. Lazarides, E. 1976. Actin, α-actinin, and tropomyosin interaction in the structural organization of actin filaments in nonmuscle cells. *J. Cell Biol.* 68:202–219.
25. Lazarides, E., and K. Burridge. 1975. α-Actinin: immunofluorescent localization of a muscle structural protein in non-muscle cells. *Cell.* 6:289–298.
26. Lazarides, E., and K. Weber. 1974. Actin antibody: the specific visualization of actin filaments in non-muscle cells. *Proc. Natl. Acad. Sci. USA.* 71:2268–2272.
27. Masaki, T., M. Embo, and S. Ebashi. 1967. Localization of alpha-actinin at Z-band. *J. Biochem. (Tokyo).* 62:630–632.
28. Pepe, F. A. 1975. Structure of muscle filaments from immunohistochemical and ultrastructural studies. *J. Histochem. Cytochem.* 23:543–562.
29. Rash, J. E., T. F. McDonald, H. G. Sachs, and J. D. Ebert. 1972. Muscle-like arrays in a fibroblast line. *Nature New Biol.* 237:160.
30. Rathke, P. C., M. Osborn, and K. Weber. 1979. Immunological and ultrastructural characterization of microfilament bundles: polygonal nets and stress fibers in an established cell line. *Eur. J. Cell Biol.* 19:40–48.
31. Robinson, T. F., and S. Winegrad. 1979. The measurement and dynamic implication of thin filament lengths in heart muscle. *J. Physiol. (Lond.).* 286:607–619.
32. Rohlick, P., and I. Olah. 1967. Cross-striated fibrils in the endothelium of the rat myometral arterioles. *J. Ultrastruct. Res.* 18:667–676.
33. Sanger, J. W. 1971. Formation of synthetic myosin filaments: influence of pH, ionic strength, cation substitution, dielectric constant and method of preparation. *Cytobiologie.* 4:450–466.
34. Sanger, J. W. 1975. Changing patterns of actin localization during cell division. *Proc. Natl. Acad. Sci. USA.* 72:1913–1916.
35. Sanger, J. W. 1975. Intracellular localization of actin with fluorescently labelled heavy

meromyosin. *Cell Tissue Res.* 161:431–444.
36. Sanger, J. W., and F. V. McCann. 1968. Ultrastructure of moth alary muscles and their attachment to the heart wall. *J. Insect Physiol.* 14:1539–1544.
37. Sanger, J. M., and J. W. Sanger. 1980. Banding and polarity of actin filaments in interphase and cleaving cells. *J. Cell Biol.* 86:568–575.
38. Sanger, J. W., J. M. Sanger, T. E. Kreis, and B. M. Jockusch. 1980. Reversible translocation of cytoplasmic actin into the nucleus caused by dimethyl sulfoxide. *Proc. Natl. Acad. Sci. USA.* 77:5268–5272.
39. Spooner, B. S., K. M. Yamada, and N. K. Wessells. 1971. Microfilaments and cell locomotion. *J. Cell Biol.* 49:595–613.
40. Sternberger, L. A. 1974. Immunocytochemistry. Prentice Hall, Inc. Englewood Cliffs, NJ.
41. Weber, K., and U. Groeschel-Stewart. 1974. Antibody to myosin: the specific visualization of myosin containing filaments in non-muscle cells. *Proc. Natl. Acad. Sci. USA.* 71:4561–4564.
42. Wehland, J., and K. Weber. 1980. Distribution of fluorescently labeled actin and tropomyosin after microinjection in living tissue culture cells as observed with TV image intensification. *Exp. Cell Res.* 127:397–408.
43. Wong, A. J., T. D. Pollard, and I. M. Herman. 1981. Endothelial cells contain stress fibers in vivo. *J. Cell Biol.* 91(2, Pt.2):299*a*. (Abstr.)
44. Wolf, E., A. Deboben, F. A. Bauta, H. Faulstich, and T. H. Wieland. 1979. Fluorescent phallotoxin, a tool for the visualization of cellular actin. *Proc. Natl. Acad. Sci. USA.* 76:4498–4502.
45. Zigmond, S. H., J. J. Otto, and J. Bryan. 1979. Organization of myosin in a submembranous sheath in well-spread human fibroblasts. *Exp. Cell Res.* 119:205–219.